Transparent Nanowire Network Electrode for Textured Semiconductors

Jinwei Gao,* Ke Pei, Tianyi Sun, Yaohui Wang, Linghai Zhang, Weijin Peng, Qinggeng Lin, Michael Giersig, Krzysztof Kempa, Zhifeng Ren, and Yang Wang*

This work presents an inexpensive and easily manufacturable, highly conductive and transparent nanowire network electrode for textured semiconductors. It is based on lines of silver nanoparticles transformed into a nanowire network by microwave or furnace sintering. The nanonetwork electrode on crystalline silicon is demonstrated experimentally, with the nanoparticles self-assembling in the valleys between the pyramids of the textured surface. Optical experiments show that this conductive nanowire network electrode can be essentially 'invisible' when covered with the conventional anti-reflection coating (ARC), and thus could be employed in photovoltaic applications.

1. Introduction

Many photovoltaic and photonic applications could benefit from anti-reflection coatings (ARCs), which not only resonantly suppress reflection, but also are very conductive. Such a need exists, for example, in the case of crystalline silicon solar cells.[1–3] At present, while excellent suppression of reflections is achieved in such solar cells by the chemical surface texturing and ARCs, a moderate conductivity of the over-doped underlying silicon requires a dense network of macroscopic metallic connecting bars.[4,5] These, in turn, shadow the active surface of the cell, compromising the efficiency.

Also, the commonly used transparent metal, indium tin oxide (ITO), cannot be used as an ARC since it would have to be much thicker than required by the ARC conditions in order to assure sufficient conduction. Metallic nanonetworks have been proposed as alternative window electrodes. These also require a compromise between conductivity and transparency, but they can be combined with the ARC film, which does not have to be conductive. In planar configurations, and on transparent, low-dielectric-constant substrates, the optical[6] and/or photovoltaic[7] performance of such nanonetworks has been comparable or slightly better than that of ITO. The importance of the dielectric environment in controlling the optical response of metallic nanoarrays has been also demonstrated.[8]

Inspired by these studies, we propose here a highly conducting, metallic nanowire network electrode (NNE) placed between an ARC and a textured crystalline silicon surface. In contrast to the conventional nanonetworks, our NNE is embedded in the valleys of the textured silicon surface, which reduces its scattering cross-section and, consequently, the reflectance. Also, placement of the NNE in between the ARC film (low dielectric constant) and silicon (large dielectric constant) improves the wave impedance matching, further reducing the reflectance. We demonstrate that our NNE combined with an ARC can suppress the reflection from a textured silicon surface as efficiently as the ARC alone, but with the added benefit of high conductivity. Our NNE is based on nanowires assembled from silver nanoparticles (NPs)

Prof. J. W. Gao, K. Pei, Y. H. Wang, L. H. Zhang, W. J. Peng, Q. G. Lin, Prof. Y. Wang
Institute for Advanced Materials (IAM)
South China Academy of Advanced Optoelectronics
South China Normal University
Guangzhou 510006, China
E-mail: gaojw@scnu.edu.cn; wangyangfs@hotmail.com

T. Y. Sun, Prof. K. Kempa, Prof. Z. F. Ren
Department of Physics, Boston College
Chestnut Hill, Massachusetts 02467, USA

Prof. M. Giersig
Institute of Experimental Physics
Freie University of Berlin
Berlin 14195, Germany
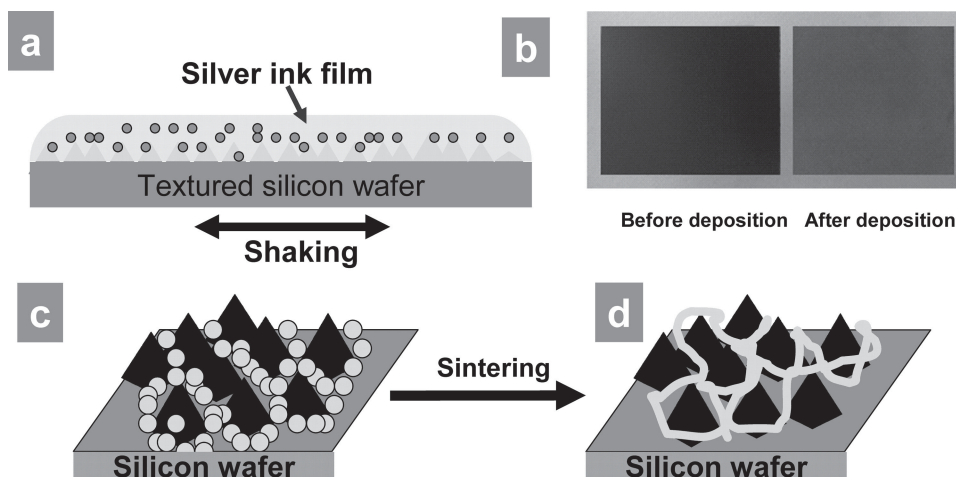
Figure 1. Schematic of the NN formation process. a) Deposition of the silver ink thin film on the tSi surface. b) Optical image of the tSi surface before (left panel) and after (right panel) NN formation. c) Agglomeration/settling of NP chains in the valleys. d) Formation of nanowires after sintering.

deposited via an inexpensive solution-based process on a textured silicon (tSi) surface, like that employed in crystalline solar cells. The transformation from the nanoparticle assembly to the NNE is achieved by microwave or furnace sintering, with the resulting nanowires formed in the 'valleys' between the microscopic pyramids of the textured morphology. This NNE could be employed as the window electrode of crystalline solar cells, with the potential for elimination (or at least substantial reduction of the number) of connecting bars.

2. Results and Discussion

2.1. Sample Preparation

The fabrication process of NNE includes three major steps: silver ink preparation, coating of the tSi surface with the ink film (**Figure 1**a), assembly/settling of NPs in the valleys between the pyramids (Figure 1c), and finally the sintering of NPs to form the NNE (Figure 1d).

The silver ink is produced by a typical wet-chemical method[9,10] with NPs of 100–200 nm in diameter. The method of thin film-coating involved in this process is a convenient and inexpensive one, similar to that extensively used in the thin film industry.[11] In this work, we deposited a thin film of silver ink onto the textured surface of a (100) silicon wafer. Within a few minutes, the nanoparticles agglomerate/settle into the 'valleys' between the pyramids (typically ~1.5 micrometers high and ~3 micrometers wide at the base). This process is enhanced with mechanical shaking of the wafer. **Figure 2** (left scanning electron microscopy (SEM) image)

shows the formation of continuous paths of touching NPs in the valleys. Such a network of NP chains forms when NP density exceeds the percolation threshold.

However, the thin insulating poly(vinylpyrrolidone) (PVP) shells covering the nanoparticles (a by-product of their synthesis) lead to large interparticle contact resistance. In order to remove these insulating PVP shells and also to physically connect (pre-melt) the touching NPs and thus to improve the electrical conductivity, we employed two sintering methods: microwave (MW) radiation and furnace annealing.[12,13] Figure 2 (right column) shows SEM images of the formed NNEs after MW (top) and furnace (bottom) sintering. The insets, which show zoomed-in sections of the
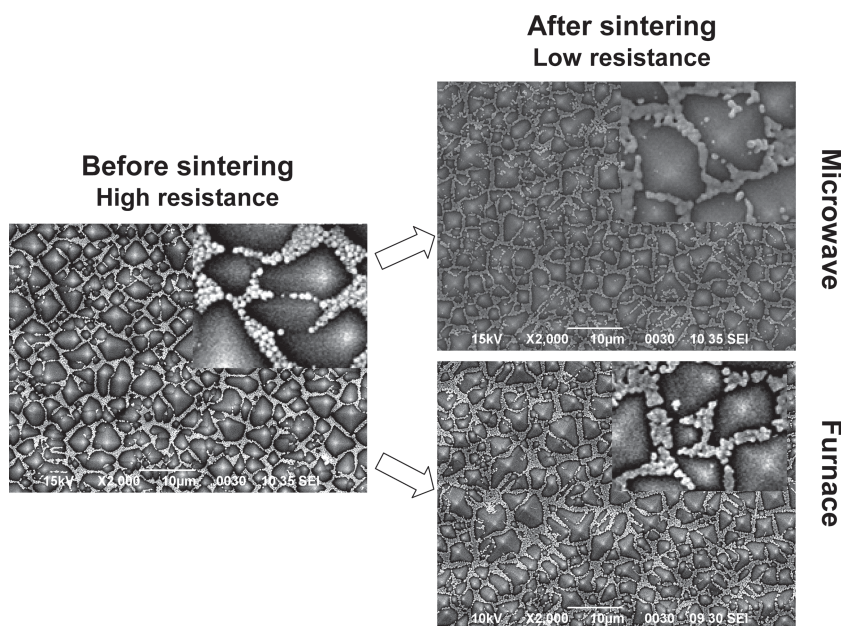
Figure 2. SEM images of the NN on textured silicon. Left panel: before sintering. Right-top panel: after MW sintering. Right-bottom panel: after furnace sintering. Insets show zoomed-in fragments of the corresponding surfaces.
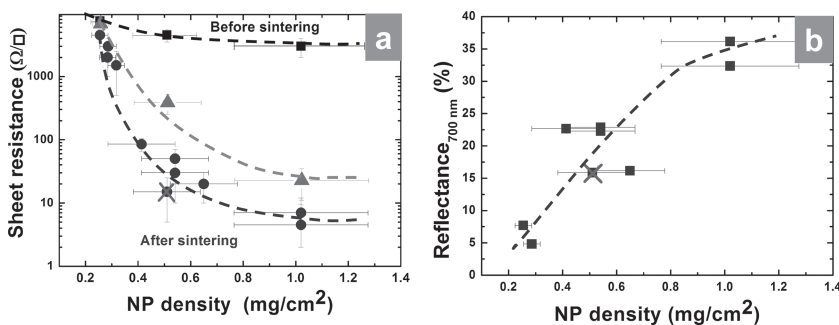
Figure 3. The electrical and optical measurements of NNE. a) Sheet resistance versus NP density: before sintering (squares), after furnace sintering (triangles), and after MW sintering (circles). b) Optical reflectance after MW sintering versus NP density. Lines in (a) and (b) are a guide for the eye, and crosses indicate the current optimal structure.

structures, clearly demonstrate strong pre-melting of NPs in the case of the MW sintering. This pre-melting is less extensive in the case of the furnace sintering. Finally, to complete the structure, we deposited a silicon nitride ARC film on top of the NNE.

2.2. Electrical Characterization of the NNE

Figure 3a shows the measured sheet resistance R_s versus the NP density for the networks before (squares), and after MW (circles) and furnace (triangles) sintering. Clearly a dramatic reduction of R_s after sintering occurs with increased NP density. Also, furnace sintering is less efficient than the MW sintering in lowering the sheet resistance, as expected from inspection of Figure 2.

2.3. Optical Characterization of NNE

Figure 3b shows that the reflectance $R_{700 \text{ nm}}$ (measured at the radiation wavelength of 700 nm) of the MW-sintered NNE increases with NP density. Therefore, there is a NP density at which a compromise can be achieved between the low resistance and large reflectance of the network. According to Figure 3, in the present set of structures this compromise results in an NNE with $R_s \approx 15 \ \Omega/\text{sq}$, and a reflectance of $R_{700 \text{ nm}} \approx 16\%$. This is indicated by crosses in Figure 3. The reflectance spectrum of this optimal network with and without an ARC, as well as that for the tSi with and without an ARC, is shown in **Figure 4**.

While the reflectance of NNE on an tSi surface is clearly larger than that for the tSi surface without a network (this agrees with the optical images in Figure 1b), the NNE reflectance (with an ARC) is essentially identical to the tSi surface with an ARC alone; this is the key result of this work.

The marginal reflectivity of the optimal NNE with an ARC (Figure 4) is not due to absorption of radiation in the nanonetwork, but to improved transmission into the silicon substrate. To demonstrate that, we first evaluate the absorption analytically, and then confirm the result by a direct measurement. Since the openings in the network are clearly macroscopic (on the order of several micrometers), while

the nanowire width is comparable to the wavelength (of the order of 1 micrometer), a good approximation should be a simple geometric formula for the total reflectance from the network,

$$R = R_0(1 - \nu) + R_m \nu \tag{1}$$

where R_0 is the reflectance without the network, and ν is the fraction of the surface area covered by the network. This immediately leads to the following expression for the total absorbance by the network,

$$A_n = \nu A_m = \nu(1 - R_m) = (1 - R_0)\nu - \Delta R \tag{2}$$

where A_m is the metallic absorbance, and $\Delta R = R - R_0$. The transmittance into silicon (TIS), defined as a transmittance, T, at the illuminated surface of silicon, is simply given by

$$T = (1 - \nu)(1 - R_0). \tag{3}$$

All required parameters needed to evaluate A_n and T have been measured: from a statistical analysis of SEM pictures (e.g., Figure 2) we obtain $\nu = 0.16$, and from Figure 4 we find for structures without any ARC that $R \approx 0.17$ and $R_0 \approx 0.11$. With these parameters, Equation (2) yields $A_n \approx 0.08$, and $T \approx 0.75$. The corresponding result for the structure with an ARC is $A_n \approx 0.15$ and $T \approx 0.8$.

To confirm these results, we have measured directly the NNE-induced change in TIS ($\Delta T = T - T_0$), in the NIR range ($\lambda = 910$–970 nm) for a structure without an ARC. In this range, the silicon substrate becomes slightly transparent, so that the change in transmission across the substrate due
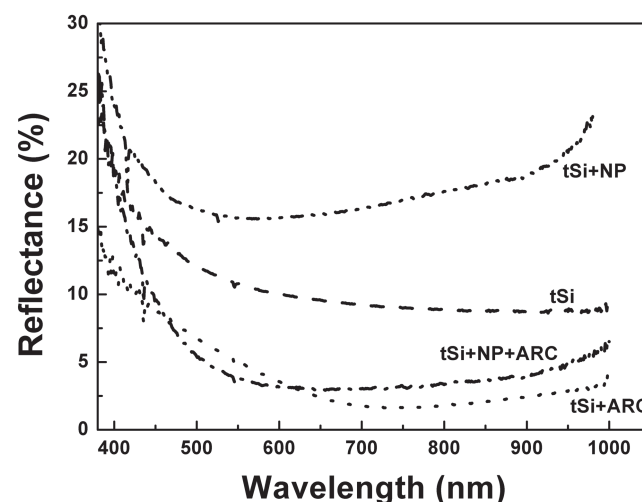
Figure 4. Reflectance spectrum of an optimal NNE (shown as crosses in Figure 3) with (tSi+NP+ARC) and without (tSi+NP) an ARC. Shown also is the reflectance of textured silicon with (tSi+ARC), and without (tSi) an ARC. Note that structures with an ARC (with or without NNE) have similar, very small reflectances.
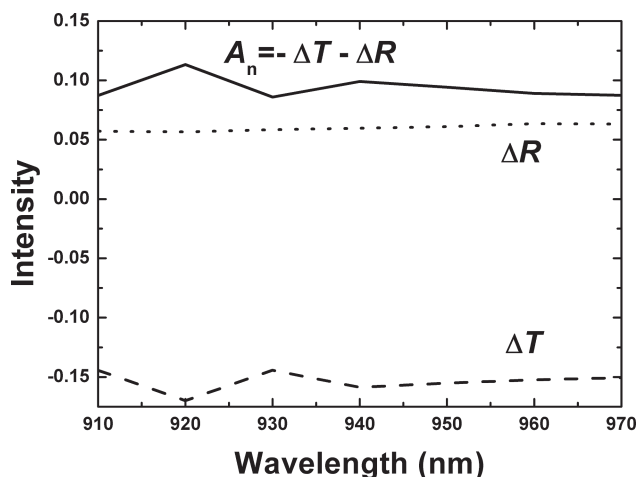
Figure 5. Absorbance of NNE (without ARC) A_n obtained from measured changes in the reflectance ΔR and transmittance ΔT induced by NNE.

to NNE, $\delta t = (t - t_0)/t_0$, can be measured, and simply related to the corresponding change in TIS (ΔT). Since the silicon absorbance at the illuminated surface is vanishingly small, $T_0 + R_0 = 1$ and $T + R + A_n = 1$. Also, since the substrate (silicon) is optically thick and lossy, its opposite surfaces are decoupled, and thus[14] $\Delta T/T_0 = \delta t$. These lead to the final expression for the NNE absorbance,

$$A_n = -\Delta T - \Delta R = -(1 - R_0)\delta T - \Delta R. \qquad (4)$$

Figure 5 shows the measured ΔT, ΔR, and the resulting A_n. Clearly, the NNE absorbance is $A_n \approx 0.09$, slightly higher that the estimate above, and in broad agreement with a recent report.[15] Further reduction of the nanonetwork absorbance will be achieved by reducing v.

The excellent optical performance of our nanonetwork is primarily due to the embedded nature of the metallic network, which causes a significant part of the reflected/scattered light from the network to be re-absorbed by the pyramids, thus enhancing the overall transmission into the silicon substrate. In addition, the refraction on the nanowires of the network is expected to further reduce the shading effect, as well as their plasmonic action similar to that involved in the extraordinary optical transmission.[16] We also note that the absorption in metallic films strongly depends on the film morphology, and can be as small as in bulk silver for rapidly deposited films, in which the granularity is minimized.[14] Recently, it has also been demonstrated that nanoscopically thin films can be made (through annealing) to have the best bulk quality.[17]

This NNE could be employed in any application which requires high transmission and high electrical conductivity and, in particular, in solar cells. The high conductivity of the NNE should allow for reduction/elimination of the macroscopic metallic connecting bars, thereby reducing/eliminating their shadowing effect. In addition, the NNE could eliminate the need for silicon overdoping, which should benefit the quality of the p–n junction. However, to successfully implement this NNE in solar cells, its performance must

be improved, as demonstrated by the results shown in Figures 3 and 4. In order to eliminate the conducting bars, the sheet resistance must be reduced by a factor of 10 to $R_s \approx 1\ \Omega/\text{sq}$, while the reflectance should remain unchanged. This can be achieved by noticing that in the current process (see Figure 2) the nanowire formation is still incomplete, with a large fraction of NPs remaining disconnected. A simple estimate shows that a more continuous NNE could achieve the required reduction of the sheet resistance with a NP density of 1 mg/cm². An additional problem that might require an improvement is the contact between the NNE and tSi.

3. Conclusion

In conclusion, we have demonstrated an inexpensive new scheme to develop a highly conductive metallic nanowire network electrode (NNE), made with silver nanoparticles self-assembled on the textured surface of a silicon substrate, and subsequently covered with a dielectric, transparent ARC. Microwave sintering of the nanoparticles has been used to convert the loose nanoparticle network into a network of nanowires occupying the valleys between the pyramids of the textured silicon surface. We show that this composite ARC (ARC plus NNE) is essentially as efficient in suppressing the reflection as the conventional ARC alone, and we demonstrate that this suppression is primarily due to increased transmission into the silicon, and not the absorbance of NNE. An improved NNE–ARC can be used to improve the crystalline silicon solar cells by eliminating (or at least reducing the need for) the conducting bars, at lower (or at least essentially the same) cost.

4. Experimental Section

Synthesis of Silver Ink: Making the nanoparticle ink involves reducing silver nitride (0.1 M) (99%, Sigma-Aldrich) in an ethylene glycol solution in the present of PVP (0.6 M) (MW ≈ 40 000, Sigma-Aldrich) at 170 °C, stirring at 2000 rpm for 30 min, where ethylene glycol is both a reducer and a solvent, and PVP is a surfactant. This is subsequently followed by centrifuging, rinsing and re-dispersing the silver nanoparticles in methanol or ethanol.

Sintering of Nanoparticles: The microwave sintering was done in a commercial microwave oven operating at 2.46 GHz, with the output power of 80 W. Typical exposure time used was ~10 s, to selectively heat and sinter the silver nanoparticles into continuous conducting nanowire networks. The furnace sintering was done in a commercial rapid thermal processor (RTP-500, Beijing Eaststar Labs) with temperature of 320 °C and duration of 10 s.

SiN Film Deposition: To deposit the dielectric film on the nanowire network we used a commercial industrial plasma-enhanced chemical vapor deposition system (PECVD) of OTP Solar (Holland), at the processing temperature of 350 °C. The refractive index of SiN is 2.06 and the thickness of the SiN film was about 90 nm, which by design should interference-suppress reflection (by interference) in the middle of the optical range.

Performance Measurements: The morphologies of samples were characterized by a commercial SEM system (JEOL JCM-5700, Tokyo, Japan). R_s of samples were measured by depositing two

parallel, narrow (2 mm wide) Au strips of length 1.5 cm, and a distance of 1 cm apart. The measured resistance was then properly related to R_s. The reflectance was measured by employing the fiber-optic spectrometer (Ocean Optics, USB 4000), and the integration sphere (Ocean Optics, FOIS-1). The IR transmission was measured with the EQE system QE-PV-Si, Oriel, Newport, USA.

Acknowledgements

[1] M. A. Green, K. Emery, Y. Hishikawa, W. Warta, E. D. Dunlop, *Prog. Photovoltaics* **2012**, *20*, 12.

[2] M. A. Green, *Solar Cells: Operating Principles, Ttechnology, and System Applications*, Prentice-Hall, Inc., Englewood Cliffs, NJ **1982**.

[3] M. A. Green, *Prog. Photovoltaics* **2009**, *17*, 183.

[4] J. Szlufcik, S. Sivoththaman, J. Nlis, R. P. Mertens, R. Van Overstraeten, *Proc. IEEE* **1997**, *85*, 711.

[5] Y. Xiu, L. Zhu, D. W. Hess, C. Wong, *Nano Lett.* **2007**, *7*, 3388.

[6] J. van de Groep, P. Spinelli, A. Polman, *Nano Lett.* **2012**, *12*, 3138.

[7] M. G. Kang, M. S. Kim, J. Kim, L. J. Guo, *Adv. Mater.* **2008**, *20*, 4408.

[8] F. J. Beck, A. Polman, K. R. Catchpole, *J. Appl. Phys.* **2009**, *105*, 114310.

[9] Y. Sun, B. Mayers, T. Herricks, Y. Xia, *Nano Lett.* **2003**, *3*, 955.

[10] Y. Sun, Y. Xia, *Science* **2002**, *298*, 2176.

[11] A. Ahmad, P. Mukherjee, S. Senapati, D. Mandal, M. I. Khan, R. Kumar, M. Sastry, *Thin Solid Films* **2003**, *28*, 313.

[12] J. Perelaer, B. J. de Gans, U. S. Schubert, *Adv. Mater.* **2006**, *18*, 2101.

[13] R. Roy, D. Agrawal, J. Cheng, S. Gedevanishvili, *Nature* **1999**, *399*, 668.

[14] O. S. Heavens, *Optical Properties of Thin Solid Films*, Dover Publications, Inc., NY **1965**.

[15] W. Chen, M. D. Thoreson, S. Ishii, A. V. Kildishev, V. M. Shalaev, *Opt. Express* **2010**, *18*, 5124.

[16] T. W. Ebbesen, H. Lezec, H. Ghaemi, T. Thio, P. Wolff, *Nature* **1998**, *391*, 667.

[17] W. Chen, M. D. Thoreson, S. Ishii, A. V. Kildishev, V. M. Shalaev, *Opt. Express* **2010**, *18*, 5124.